U.S. DEPARTMENT OF ENERGY

PNNL-20747

Prepared for the U.S. Department of Energy
under Contract DE-AC05-76RL01830

Ostwald Ripening and Its Effect on PuO_2 Particle Size in Hanford Tank Waste

CH Delegard

September 2011

Pacific Northwest
NATIONAL LABORATORY

Proudly Operated by Battelle *Since 1965*

DISCLAIMER

PACIFIC NORTHWEST NATIONAL LABORATORY
operated by
BATTELLE
for the
UNITED STATES DEPARTMENT OF ENERGY
under Contract DE-AC05-76RL01830

Printed in the United States of America

Available to DOE and DOE contractors from the
Office of Scientific and Technical Information,
P.O. Box 62, Oak Ridge, TN 37831-0062;
ph: (865) 576-8401
fax: (865) 576-5728
email: reports@adonis.osti.gov

Available to the public from the National Technical Information Service
5301 Shawnee Rd., Alexandria, VA 22312
ph: (800) 553-NTIS (6847)
email: orders@ntis.gov <http://www.ntis.gov/about/form.aspx>
Online ordering: http://www.ntis.gov

This document was printed on recycled paper.
(8/2010)

PNNL-20747

Ostwald Ripening and Its Effect on PuO_2 Particle Size in Hanford Tank Waste

CH Delegard

September 2011

Prepared for
the U.S. Department of Energy
under Contract DE-AC05-76RL01830

Pacific Northwest National Laboratory
Richland, Washington 99352

Abstract

Between 1944 and 1989, 60 percent (54.5 metric tons) of the United States' weapons-grade plutonium and an additional 12.9 metric tons of fuel-grade plutonium were produced at the Hanford Site in southeastern Washington State. High-activity wastes, including plutonium lost from the separations processes used to isolate the plutonium and subsequent plutonium recycle processes, were discharged to underground storage tanks during these operations. Plutonium in the Hanford tank farms is estimated to amount to ~700 kg but may be up to ~1000 kg. Despite these apparent large quantities, the average plutonium concentration in the ~200 million liter tank waste volume averages only about 0.003 grams per liter (or ~0.0002 wt%). The plutonium is largely associated with low-solubility metal hydroxide/oxide sludges where its low concentration and intimate mixture with neutron-absorbing elements (e.g., iron) are credited in nuclear criticality safety. However, concerns have been expressed that plutonium, in the form of plutonium hydrous oxide, $PuO_2 \cdot xH_2O$, could undergo sufficient crystal growth through Ostwald ripening in the alkaline tank waste to potentially be separable from neutron absorbing constituents by settling or sedimentation. It was found through thermodynamic considerations and laboratory studies of chemically analogous systems that plutonium that entered the alkaline tank waste by precipitation through neutralization from acid solution likely is present as 2- to 3-nm (0.002- to 0.003-μm) $PuO_2 \cdot xH_2O$ crystallite particles that grow from that point at exceedingly slow rates, thus posing no risk to physical segregation. These conclusions are reached by both general considerations of Ostwald ripening and specific observations of the behavior of $PuO_2 \cdot xH_2O$ upon aging in alkaline solution.

Acknowledgments

This work was performed for Washington River Protection Solutions under the direction of Jacob Reynolds. The author acknowledges the contributions of Dan Herting, Washington River Protection Solutions, to the initial thoughts in the introduction to this report, the observations and discussions on plutonium hydrous oxide aging phenomena made by Alexandre Yusov and colleagues of the Institute of Physical Chemistry and Electrochemistry of the Russian Academy of Sciences, Moscow, the suggestion made by Roy Wymer (private consultant) that diffusion may be controlling plutonium concentration changes in solution, and the careful technical review of the paper made by Sergey Sinkov of Pacific Northwest National Laboratory (PNNL). The work at PNNL was led by Susan Jones and the report edited by Susan Ennor.

Acronyms and Abbreviations

°C	degree(s) Celsius
J	joule(s)
K	temperature in Kelvin
kJ	kilojoule(s)
µm	micron(s)
M	molar concentration
NaOH	sodium hydroxide
nm	nanometer(s)
PuO_2	plutonium dioxide
$PuO_2 \cdot xH_2O$	plutonium(IV) hydrous oxide
wt%	weight percent
XRD	X-ray diffraction

Contents

Abstract iii
Acknowledgments v
Acronyms and Abbreviations vii
1.0 Introduction 1
1.1 Plutonium Disposition in Hanford Tank Waste 1
1.2 Ostwald Ripening 2
1.3 Report Contents and Organization 3
2.0 Effect of Aging on $PuO_2 \cdot xH_2O$ Particle Size 3
3.0 Effect of Temperature on $PuO_2 \cdot xH_2O$ Particle Size 7
4.0 References 9
Appendix A – Derivation of Equations for the Effect of PuO_2 Particle Size on PuO_2 Solubility Product and Solubility A.1
Appendix B – XRD Patterns of $PuO_2 \cdot xH_2O$ Precipitated from Pu(IV) and Pu(VI) Nitrate Solution in NaOH Solution B.1
Appendix C – Sodium Hydroxide Solution Viscosities and Fluidities as Functions of Concentrations and Temperature C.1

Figures

1 $PuO_2 \cdot xH_2O$ Particle Size, d_t, as a Function of Decrease in Solubility from That of the Birth Particle 6
2 Plutonium Concentrations Above Solids Precipitated from Pu(IV) Nitrate in Room-Temperature NaOH Solutions as a Function of Time 6
3 Predicted and Observed $PuO_2 \cdot xH_2O$ Particle Sizes in NaOH Solution as Functions of Time 7

1.0 Introduction

The study reported here was performed for Washington River Protection Solutions to examine the phenomenon of Ostwald ripening as it applies to plutonium(IV) hydrous oxide—$PuO_2 \cdot xH_2O$—and to derive conclusions about the rate of $PuO_2 \cdot xH_2O$ particle growth in Hanford Site tank waste.

1.1 Plutonium Disposition in Hanford Tank Waste

Between 1944 and 1989, the Hanford Site in Washington State produced 54.5 metric tons or 60 percent of the plutonium for the United States weapons program and produced an additional 12.9 metric tons of fuels-grade plutonium. The fabrication of the uranium metal fuel, its irradiation in eight production reactors and one dual-purpose production/power reactor, and reprocessing of the irradiated fuel to extract the product plutonium and to recover the uranium all occurred at Hanford. Hanford also recovered and purified plutonium scrap from its own and from other weapons complex sources, converted the plutonium to metal, and, from 1949 until 1965, fabricated plutonium metal into shapes for nuclear weapons (Briggs 2001). The higher activity waste solutions from the chemical processing and manufacturing operations were discharged to underground waste storage tanks with lower activity solutions discharged to the ground and solid waste residues placed in drums for burial and for shipment to the Waste Isolation Pilot Plant.

Hanford used three reprocessing technologies to recover the plutonium from about 100,000 metric tons of irradiated uranium metal fuel—the bismuth phosphate (B and T Plants, 1944–1956), REDOX (1951–1968), and PUREX (1956–1971, 1983–1989) processes. High-activity wastes, including plutonium process losses from these operations, were discharged to the underground storage tanks. Operations at the Plutonium Finishing Plant (1949–2004) also produced plutonium-bearing chemical process wastes but only sent those wastes to the tank farms from 1973 onward. A best-basis estimate of plutonium quantities lost to the tank wastes is 672 kg (Kupfer et al. 1999) but conservative loss estimates range as high as 981 kg (Roetman et al. 1994). Despite these apparent large quantities, the average plutonium concentration in the ~55 million gallon (~200 million liter) volume of tank waste is only about 0.003 grams per liter (~0.0002 wt%) or about 1.4×10^{-5} M using best-basis loss values.

The chemical disposition of plutonium in Hanford Site tank wastes has been studied via focused investigation of actual wastes and via more general studies of the behavior of plutonium in alkaline media characteristic of, or near the compositions of, actual waste. The results of these studies have been summarized in the context of the Hanford process waste origins. Most of the plutonium loss streams were in nitric acid solution mixed with much greater concentrations of other elements (e.g., iron, aluminum, chromium, uranium). When the acid wastes were made alkaline with sodium hydroxide before discharge to the mild steel-lined underground storage tanks and then concentrated by evaporation, dissolved and crystalline sodium nitrate, excess sodium hydroxide solution, and low-solubility metal oxide, hydroxide, and hydrous oxide sludges were formed with the plutonium dispersed on an atomic scale within the low-solubility sludges (Barney and Delegard 1999). In the presence of only sodium hydroxide, or even accompanied by most other anions, dissolved plutonium precipitates from nitric acid solution to form a low-solubility $PuO_2 \cdot xH_2O$ solid phase. However, with the more abundant iron and other polyvalent metals also present, plutonium disperses by coprecipitation into the bulk metal (hydr)oxide or hydrous oxide sludges, showing particularly high affinity for the iron phases (Fedoseev et al. 1998).

Despite these conditions, concern has been raised that some of the plutonium may not have coprecipitated or, if it was, it could have become disassociated from the bulk host metal (hydr)oxides through hydrothermal recrystallization processes. The resulting $PuO_2 \cdot xH_2O$ then might grow in particle size due to the phenomenon known as Ostwald ripening to form dehydrated and increasingly larger crystals of plutonium dioxide, PuO_2. Because of the ~11 g/cm^3 density of PuO_2 and the growing PuO_2 particle size, hydrodynamic forces imposed by tank operations and natural processes (pumping, mixing, convection, settling) then potentially could segregate the PuO_2 and challenge criticality safety by allowing the plutonium particles to collect in a more concentrated and compact form without the co-location of accompanying neutron absorbers (chiefly iron) otherwise found abundantly in the tank waste.

1.2 Ostwald Ripening

Ostwald ripening is a process by which small particles dissolve, due to their enhanced solubility arising from their high surface area and energy, and larger particles grow to result in a "coarsening" of the solid particle or an overall increase in the mean particle size (Liu et al. 2007). Ostwald ripening is *not* expected to occur to a significant extent for PuO_2 or $PuO_2 \cdot xH_2O$ particles in alkaline Hanford tank waste. Instead, any micron-scale crystalline plutonium oxide found in the tank waste almost certainly entered the tank in that form and, because of the low solubility of plutonium phases in alkaline media, was not formed by processes within the tank. As will be shown, plutonium that entered the alkaline tank waste by precipitation through neutralization from acid solution likely is present as $PuO_2 \cdot xH_2O$ crystallite particles at the 2- to 3-nm (0.002- to 0.003-μm) scale. The crystallites grow from that point at exceedingly slow rates. These conclusions are reached by both general considerations of the phenomenon of Ostwald ripening and specific observations of the behaviors of PuO_2 and $PuO_2 \cdot xH_2O$ upon aging in alkaline solution.

In general, a precipitate/solvent system at saturation appears to be static, but is in fact dynamic, with both dissolution and crystallization of the precipitate occurring simultaneously and at the same or nearly the same rate. Ostwald ripening occurs because the solubility of the smaller precipitate particles is greater than the solubility of the larger particles. The smaller particles have higher specific surface area than the larger particles and thus a greater proportion of the imperfect crystal structure that is present at the solid-solution interface. As a result of their greater solubility, the smaller particles tend to dissolve and their solutes deposit onto the surfaces of the larger and less soluble particles.

The rate of crystal growth by Ostwald ripening is proportional to the solubility of the precipitate as described mathematically by Liu and colleagues (2007; and many other references). For precipitates with very low solubility, like PuO_2, the rates of dissolution and crystallization are so slow that re-distribution of particle sizes due to Ostwald ripening may take place only on geologic time scales, not over the time scale of tank waste storage. An example cited in the literature (Lee et al. 2005) states that "Ostwald ripening is not an important mechanism for tin oxide systems, as expected by the low solubility of this oxide." Another example states that "In a sol of a highly insoluble substance, such as silver iodide hydrosol, this phenomenon [Ostwald ripening] will be of little consequence, since both large and small particles have extremely little tendency to dissolve" (Shaw 1980).

The potential growth of PuO_2 particles by Ostwald ripening is further attenuated in Hanford tank waste sludges, which contain abundant low-solubility metal hydroxide surfaces, such as those of ferric hydroxide, that have high affinity for plutonium, thus lowering plutonium's effective concentration, while

the metal hydroxide particles themselves provide physical barriers that impede dissolved plutonium from diffusing from the smaller and dissolving PuO_2 particles to the growing PuO_2 particles.

1.3 Report Contents and Organization

The effects of aging on $PuO_2 \cdot xH_2O$ particle growth are examined in Section 2.0 and the effects of temperature on $PuO_2 \cdot xH_2O$ particle growth are examined in Section 3.0. Section 4.0 contains a list of the references cited in the main text and appendixes of this report. The technical background for predicting $PuO_2 \cdot xH_2O$ particle size, the measurements of $PuO_2 \cdot xH_2O$ particle size for materials aging in alkaline solution, and the influence of solution fluidity on the solute diffusion rates, which control the Ostwald ripening particle growth rate, are discussed in the appendices.

2.0 Effect of Aging on $PuO_2 \cdot xH_2O$ Particle Size

Information about the rate of Ostwald ripening of $PuO_2 \cdot xH_2O$ can be deduced from results of long-term studies of the plutonium concentrations observed in alkaline solution of variable sodium hydroxide (NaOH) concentration containing $PuO_2 \cdot xH_2O$, created by making plutonium nitrate solutions alkaline in NaOH solution, and by published knowledge of the effects of aging on the solubilities of $PuO_2 \cdot xH_2O$ and fully crystalline PuO_2. According to the work of Schindler (1967), later extended to understanding the solubility of thorium(IV) oxide/hydroxide according to particle size (Bundschuh et al. 2000; Fanghänel and Neck 2002[1]), the solubility products of colloidal particles present at time t, $K_{sp}^{t}(\text{colloid})$, and fully crystallized large crystals, $K_{sp}^{0}(\text{large crystal})$, of the same chemical composition and structure are related to the size, d_t, of the colloidal particles at time t by Equation (1) (derivation shown in Appendix A):

$$\log K_{sp}^{t}(\text{colloid}) - \log K_{sp}^{0}(\text{large crystal}) = \frac{y}{d_t\ (\text{nm})} \tag{1}$$

The value of y is a function of the molecular weight of the solid (PuO_2 in the present case), PuO_2 particle density, the radii of the constituent Pu^{4+} and O^{2-} ions, and the surface area-to-volume ratio factor of 6 for the assumed spherical $PuO_2 \cdot xH_2O$ colloidal particles of diameter d_t. As shown in Appendix A, the value of y for PuO_2 is 18.46 nm.

Critically reviewed values of $K_{sp}^{0}(\text{large crystal})$ for crystalline PuO_2, $PuO_{2\,(cr)}$, and $K_{sp}^{0}(\text{colloid})$, for the amorphous hydrous oxide of PuO_2 initially formed before significant aging has occurred, $PuO_{2\,(am,hydr.)}$ or $PuO_2 \cdot xH_2O$, are $10^{-64.04}$ and $10^{-58.33}$, respectively (Guillaumont et al. 2003). By input of values for y, $K_{sp}^{0}(\text{large crystal})$, and $K_{sp}^{0}(\text{colloid})$ to Equation (1), the birth size, d_0, of the freshly formed $PuO_2 \cdot xH_2O$ particle may be determined as shown in Equations (2) and (3).

$$\log K_{sp}^{0}(\text{colloid}) - \log K_{sp}^{0}(\text{large crystal}) = -58.33 + 64.04 = 5.71 = \frac{18.46}{d_0\ (\text{nm})} \tag{2}$$

[1] Note that Th(IV) is chemically analogous to the Pu(IV) system.

$$d_0\ (\text{nm}) = \frac{18.46}{5.71} = 3.2\ \text{nm} \tag{3}$$

The d_0 = 3.2-nm birth size of $PuO_2 \cdot xH_2O$ predicted by this analysis compares closely with the 3-nm size observed for $PuO_2 \cdot xH_2O$ solids precipitated with ammonium hydroxide and then air-dried at 70°C as measured by X-ray diffraction (XRD) reflection line broadening in early Manhattan Project work (Westrum 1949). It is also close to the 2.5-nm particle size for $PuO_2 \cdot xH_2O$ precipitated by neutralizing Pu(IV) nitrate from alkaline solution after 5 hours of aging at room temperature and also for $PuO_2 \cdot xH_2O$ obtained by 2 hours of aging at 75°C (Yusov et al. 2000). The particle size in the tests by Yusov and colleagues (2000) was measured by XRD line broadening from the 111 plane appearing at 28.55° 2-θ. The research also found that the NaOH concentration (at 0.1, 1, and 10 M) had a negligible effect on particle size in tests done with 2 hours of 75°C aging. Preparation of the $PuO_2 \cdot xH_2O$ under 180–200°C hydrothermal conditions produced larger 4.5-nm particles.

Tests were done in the ~1983–1987 time frame to study the dissolution and precipitation reactions of plutonium in alkaline solution (Delegard 1985). Previously unpublished results from those tests include XRD patterns of $PuO_2 \cdot xH_2O$, prepared by precipitating plutonium nitrate solutions in NaOH solution, at various aging times. The XRD line broadening of the $PuO_2 \cdot xH_2O$ produced by precipitating Pu(IV) nitrate in 5 M NaOH solution and separated after 4 days of room temperature aging for the 111 plane reflection at 28.55° 2-θ indicates a particle size of ~2.1 nm (estimated using the Scherrer equation[1]) compared with the 3.2-nm birth size predicted by the thermodynamic analysis shown in Equation (3) and the 2.5-nm $PuO_2 \cdot xH_2O$ particle size measured by Yusov and colleagues (2000). With ~14 months of aging under room temperature (~22°C) 5 M NaOH, the $PuO_2 \cdot xH_2O$ particles prepared from Pu(IV) nitrate increased size marginally to ~2.6 nm as shown by the slight narrowing of the 28.55° 2-θ peak. The broad XRD diffraction patterns found in 5 M NaOH after 14 months were also observed for $PuO_2 \cdot xH_2O$ prepared from Pu(IV) nitrate in 2 M and 10 M NaOH and aged 14 months. After ~38 months of aging, the particle size of $PuO_2 \cdot xH_2O$ isolated from NaOH solution was ~3.0 nm.

Greater particle size was observed for $PuO_2 \cdot xH_2O$ prepared by precipitating Pu(VI) nitrate in 1 M NaOH and aged about 9½ months. In this case the particle size was about 11 nm as determined by XRD line broadening. The greater particle size shown for the Pu(VI)-origin material is attributed to the higher concentration of the dissolved plutonium, present largely as Pu(VI), compared with the Pu(IV) present in the other testing. The higher dissolved plutonium concentration present while the more soluble Pu(VI) was being radiolytically reduced to the much less soluble Pu(IV) allowed slower precipitation and greater growth to occur on the developing $PuO_2 \cdot xH_2O$ particles. The $PuO_2 \cdot xH_2O$ XRD patterns for particles prepared from Pu(IV) nitrate in 5 M NaOH after 4 days and 14 months, from Pu(IV) nitrate in NaOH at 38 months, and from Pu(VI) nitrate in 1 M NaOH after 9½ months aging are shown in Appendix B.

---

[1] $$d(\text{nm}) = \frac{K \times \lambda}{\beta \times \cos\theta} = \frac{0.9 \times 0.154\ \text{nm}}{\beta\ (\text{radians}, 2\theta) \times \cos(0.249\ \text{radians})} = \frac{0.9 \times 0.154\ \text{nm}}{\beta\ (\text{radians}, 2\theta) \times 0.969}$$

where
- K = a shape factor (typically around 0.9)
- λ = the wavelength of the copper Kα X-ray (0.154056 nm)
- β = the full width, in radians, 2-θ, at the half maximum of (in this case) the 111 plane diffraction peak at 28.55° 2-θ
- θ = the Bragg angle (28.55°/2 or 0.249 radians) of the 111 plane diffraction peak.

Other studies showed that freshly formed $PuO_2 \cdot xH_2O$ particles (aged <1 hour) prepared by addition of 10 to 130 g/L Pu(IV) in 1 to 3 M nitric acid to excess ammonium hydroxide solution (pH ~12) were less than 2 nm as estimated by electron micrography (Haire et al. 1971). The precipitates were better defined and more discrete after washing to pH 6 to 8 followed by 4 hours of reflux at 95°C to 100°C. The particles had the XRD pattern of PuO_2 while XRD line broadening showed the particle size to be less than 2.5 nm.

Overall, the published laboratory findings, previously unpublished XRD measurements from other studies, and theoretical predictions indicate that the $PuO_2 \cdot xH_2O$ birth particles produced by making Pu(IV) nitrate solution alkaline are about 2 to 3 nm in diameter.

Particle size is expected to increase with aging by Ostwald ripening. According to Equation (1), this aging is reflected in the decreased solubility product, $K_{sp}^{t}(\text{colloid})$, of the growing particle as the aging time, t, increases. As shown in Appendix A, the aging colloid's influence is also reflected in the colloid's decreased solubility (i.e., plutonium concentration, $K_{s,4}^{t}(\text{colloid})$) according to Equation (4).

$$\log K_{s,4}^{t}(\text{colloid}) - \log K_{s,4}^{0}(\text{large crystal}) = 5.71 + \log \Delta(\text{solubility}) = \frac{18.46}{d_t\ (\text{nm})} \tag{4}$$

The relationship of the change in $PuO_2 \cdot xH_2O$ particle size as solubility decreases given in Equation (4) is illustrated in Figure 1. For example, a 100-fold decrease in plutonium solubility from that of a 3.2-nm birth particle indicates that the $PuO_2 \cdot xH_2O$ particle should have grown to ~5.0 nm as shown in Equations (5) and (6).

$$\log K_{s,4}^{t}(\text{colloid}) - \log K_{s,4}^{0}(\text{large crystal}) = 5.71 + \log \Delta(\text{solubility}) = 5.71 - 2.00 = \frac{18.46}{d_t\ (\text{nm})} \tag{5}$$

$$d_t\,(\text{nm}) = \frac{18.46}{5.71 - 2.00} = 5.0\ \text{nm} \tag{6}$$

The effect of aging time on the plutonium concentration above $PuO_2 \cdot xH_2O$ in NaOH solution at room temperature (~22°C) has been studied (Delegard 1985). The results in Figure 2 show that the plutonium concentration increases with NaOH concentration but, for any given NaOH concentration, decreases in proportion to the square root of time (i.e., $t^{1/2}$) beyond a few days of aging. The decreasing plutonium concentration is observed from the initial 2-day sampling time for 1 M NaOH and from 7 days onward for all concentrations less than 9 M NaOH. The decreases in plutonium concentration continued through the end of testing at about 2 years for solutions ranging from 1 to 10 M NaOH. The decreasing plutonium concentration evidently is caused by aging or Ostwald ripening of the initial ~2–3-nm $PuO_2 \cdot xH_2O$ birth particles as they grow.

Because of the $t^{1/2}$ dependence, a ~10-fold plutonium concentration decrease is observed between the sampling performed at 7 days and the last samplings done about 100 times later at 768 or 877 days (at 3 and 4 M NaOH) for tests run at 1 M to 8 M NaOH. Conservatively, an additional 10-fold concentration decrease might occur with a further 100-fold increase of aging time. Thus, if aging time were extended another factor of 100 from 800 days to 80,000 days or ~220 years, the plutonium concentration would decrease by an additional factor of 10.

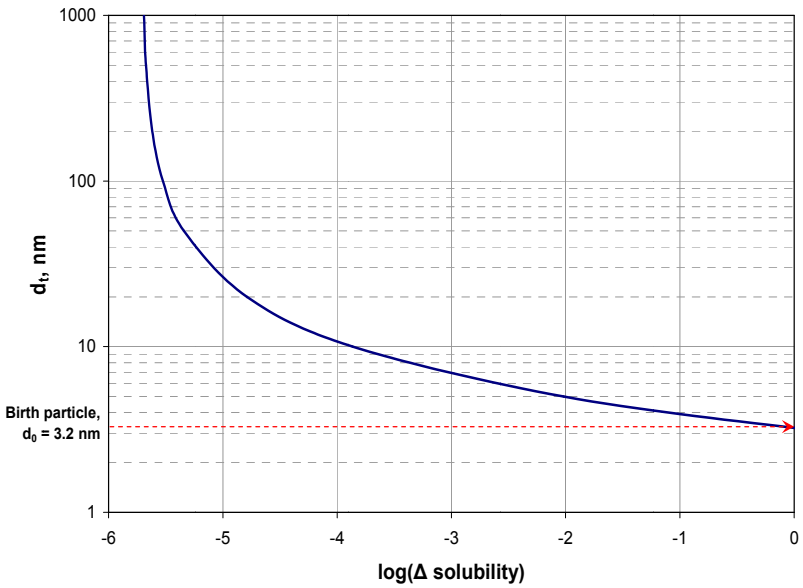

Figure 1. $PuO_2 \cdot xH_2O$ Particle Size, d_t, as a Function of Decrease in Solubility from That of the Birth Particle

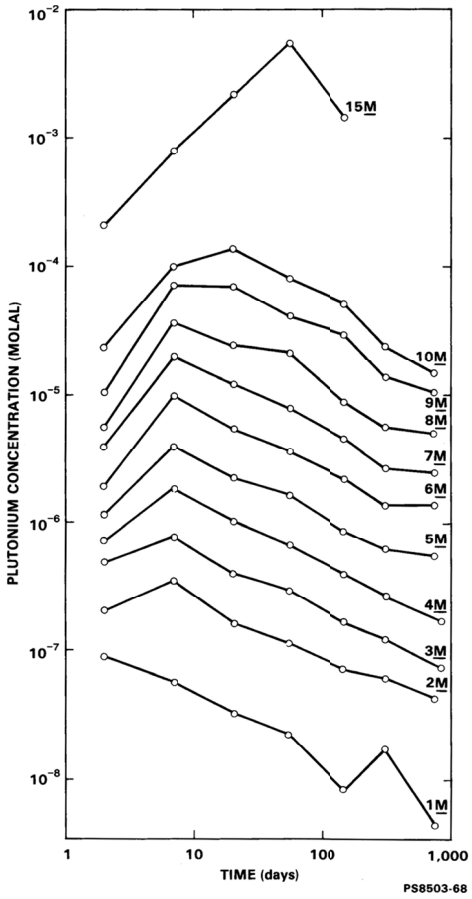

Figure 2. Plutonium Concentrations Above Solids Precipitated from Pu(IV) Nitrate in Room-Temperature NaOH Solutions as a Function of Time (Delegard 1985)

Therefore, as much as a 100-fold decrease in plutonium concentration is projected to occur after 220 years of ~22°C (room temperature) aging from the time of tank discharge as nominal 3.2-nm $PuO_2 \cdot xH_2O$ birth particles. This extended aging would attain a projected terminal particle size of only ~5.0 nm as seen in Equation (6) and illustrated in Figure 3. The $PuO_2 \cdot xH_2O$ particle sizes observed at 4 days, 14 months, and 38 months by XRD line broadening of the 111 plane appearing at 28.55° 2-θ are shown for comparison in Figure 3. The slow increase in $PuO_2 \cdot xH_2O$ particle size with time due to Ostwald ripening thus is illustrated through both thermodynamic analyses of PuO_2 and $PuO_2 \cdot xH_2O$ solubility data and direct laboratory observation.

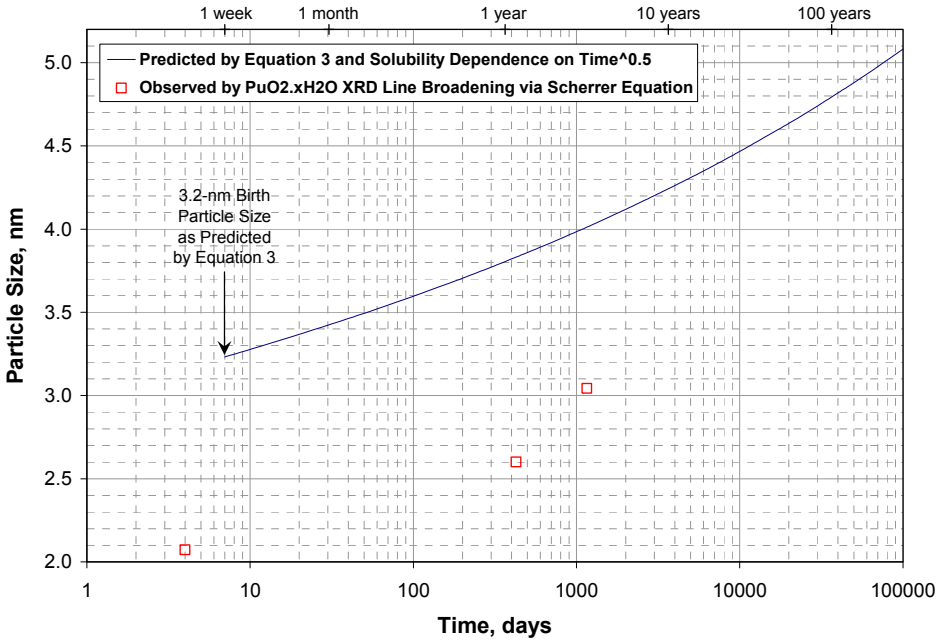

Figure 3. Predicted and Observed $PuO_2 \cdot xH_2O$ Particle Sizes in NaOH Solution as Functions of Time

3.0 Effect of Temperature on $PuO_2 \cdot xH_2O$ Particle Size

The work by Yusov and colleagues (2000) showed that moderate increase in $PuO_2 \cdot xH_2O$ particle size occurred with increasing preparation temperature. Thus, 2.5-nm particles were found after 5 hours of room temperature aging and 2 hours of 75°C aging while 4.5-nm particles were produced at 160–200°C (aging time not given). The effect of temperature on the growth of $PuO_2 \cdot xH_2O$ particles in Hanford tank waste is of interest because the waste has undergone and continues to undergo heating by both radiolytic and evaporative concentration processes. However, aside from the tests of Yusov and colleagues (2000), no explicit tests of the effects of temperature and time on $PuO_2 \cdot xH_2O$ particle size in alkaline media have been performed.

The data shown in Figure 2 provide some information about the rate of $PuO_2 \cdot xH_2O$ particle growth at room temperature (~22°C) through the rate of plutonium concentration change. The concentration dependence on $t^{½}$ can be interpreted to mean that the reaction is controlled by diffusion. In this case, the $t^{½}$ dependence of plutonium concentration found above the aging $PuO_2 \cdot xH_2O$ particles implies that the

crystallization reaction is controlled by the diffusion rate of plutonium through solution from the dissolving $PuO_2 \cdot xH_2O$ particles to the $PuO_2 \cdot xH_2O$ particles growing by Ostwald ripening.

The diffusion rate of solutes, such as dissolved plutonium, through solution is known to increase with increasing temperature (Adamson 1979). Furthermore, the diffusion rate increase with temperature occurs because of increasing solution fluidity where fluidity is inverse viscosity. Therefore, the rate of the crystallization reaction should increase at higher temperature in proportion to the corresponding increase in the solution fluidity.

The dependence of the solution fluidity on temperature follows an Arrhenius relationship in which the logarithm of the fluidity increases in proportion to the inverse absolute temperature (Adamson 1979). The activation energies calculated for aqueous solution fluidity are low compared to activation energies typically found for chemical reactions meaning that the temperature dependence of fluidity and, by extension, solute diffusion also is low. For pure water, the activation energy for fluidity is 15.8 kJ/mole. At this activation energy, the fluidity of water increases by about a factor of 2.5 by raising the temperature from 22°C (room temperature) to 70°C and by a factor of 3.4 when the temperature is raised from 22°C to 90°C. In contrast, chemical reaction rates typically increase about 2-fold for every 10°C temperature increase. Therefore, a reaction temperature increase from 22°C to 90°C would characteristically increase chemical reaction rates by a factor of about 100.

Sodium hydroxide solutions have higher viscosities than water and also have higher fluidity activation energies. In addition, both viscosity and fluidity activation energies increase with increasing NaOH concentration. These properties of NaOH solution are described in Appendix C. It is noted that NaOH is the dominant contributor to the viscosity of tank waste solution with sodium aluminate having a lesser contribution. The other constituent tank waste solutes (e.g., sodium nitrate and nitrite, $NaNO_3$ and $NaNO_2$) having little supplemental influence on viscosity.

As seen in Appendix C, the fluidity activation energy for 3 M NaOH is ~17 kJ/mole and the fluidity increases by about a factor of 2.7 between 22°C and 70°C, the temperature at the high end of typical waste vacuum evaporation operations. However, boiling temperatures also have been experienced for some tanks due to radiolytic heating. The fluidity of 3 M NaOH increases by about a factor of 3.7 between 22°C and 90°C. For 8 M NaOH (i.e., at the high end of tank waste salt concentration), the activation energy for fluidity is ~25 kJ/mole and the fluidity increases by a factor of 4.1 between 22°C and 70°C and by a factor of 6.7 between 22°C and 90°C.

As a first approximation, the higher waste storage temperatures increase NaOH solution fluidity, and thus increase the rate of $PuO_2 \cdot xH_2O$ particle growth, by about a factor of 5. It was seen in Section 2.0 that the 100-fold decrease in plutonium concentration projected to occur after 220 years of ~22°C (room temperature) aging would grow the 3.2-nm $PuO_2 \cdot xH_2O$ birth particles to ~5.0 nm. Therefore, the approximately 5-fold more rapid aging that would occur at actual tank waste temperatures and fluidities would decrease the time to attain the ~5.0 nm particle size about 5-fold to about 220/5 = 44 years.

Based on this analysis, the higher tank waste storage temperatures would elicit only marginal additional progress toward transforming the $PuO_2 \cdot xH_2O$ solids to micron-scale particles by Ostwald ripening. The $PuO_2 \cdot xH_2O$ particles still would grow by Ostwald ripening to no greater than tens of nanometers in size even after decades of hydrothermal aging.

4.0 References

Adamson AW. 1979. Pages 280–282 and 616 of *A Textbook of Physical Chemistry*, 2nd edition, Academic Press, New York.

Barney GS and CH Delegard. 1999. "Chemical Species of Plutonium in Hanford Site Radioactive Tank Wastes." Pages 83-110 of *Actinide Speciation in High Ionic Strength Media*, DT Reed, SB Clark, and L Rao (eds.), Springer Publishing Company, New York.

Briggs JD. 2001. *Historical Time Line and Information about the Hanford Site Richland, Washington*. PNNL-13524, Pacific Northwest National Laboratory, Richland, Washington. Available at: http://www.pnl.gov/main/publications/external/technical_reports/PNNL-13524.pdf.

Bundschuh T, R Knopp, R Müller, JI Kim, V Neck, and Th Fanghänel. 2000. "Application of LIBD to the Determination of the Solubility Product of Thorium(IV)-Colloids." *Radiochimica Acta* 88:625–629.

Clark DL, SS Hecker, GD Jarvinen, and MP Neu. 2006. "Plutonium." Page 936, Chapter 7, in *The Chemistry of the Actinide and Transactinide Elements*, 3rd edition, LR Morss, NM Edelstein, J Fuger, and JJ Katz (eds.), Springer, Dordrecht, The Netherlands.

Clark SB and C Delegard. 2002. "Plutonium in Concentrated Solutions." Chapter 7 in *Advances in Plutonium Chemistry 1967-2000*, DC Hoffmann, Senior Editor, American Nuclear Society, La Grange Park, Illinois.

Delegard CH. 1985. *Solubility of $PuO_2 \cdot xH_2O$ in Alkaline Hanford High-Level Waste Solution*. RHO-RE-SA-75 P, Rockwell Hanford Operations, Richland, Washington. Available at: www.osti.gov/bridge/servlets/purl/5402793-8aDMm2/5402793.pdf. Also found as "Solubility of $PuO_2 \cdot xH_2O$ in Alkaline Hanford High-Level Waste Solution," CH Delegard, 1987, *Radiochimica Acta* 41:11–21.

Dow. 2011. "Viscosity Table for Pure (Salt Free) Caustic Soda Solution." Form No. 102-00394-1203. The Dow Chemical Company. Available at: http://www.dow.com/webapps/lit/litorder.asp?filepath=causticsoda/pdfs/noreg/102-00394.pdf&pdf=true. For supplementary viscosity data, see https://tecci.bayer.de/io-tra-pro/emea/de/docId-2857611/Caustic_soda_solution.pdf.

Fanghänel Th and V Neck. 2002. "Aquatic Chemistry and Solubility Phenomena of Actinide Oxides/Hydroxides." *Pure and Applied Chemistry* 74(10):1895–1907.

Fedoseev, AM, NN Krot, NA Budantseva, AA Bessonov, MV Nikonov, MS Grigoriev, AYu Garnov, VP Perminov, and LN Astafurova. 1998. *Interaction of Pu(IV,VI) Hydroxides/Oxides with Metal Hydroxides/Oxides in Alkaline Media*. PNNL-11900, Pacific Northwest National Laboratory, Richland, Washington. Available at: http://www.osti.gov/bridge/servlets/purl/665966-ij8eO9/webviewable/665966.pdf. See also:

- Fedoseev AM, NA Budantseva, MV Nikonov, and MS Grigor'ev. 2000. "Interaction of Pu(IV) Hydroxide with Hydroxides of Some *d* and *f* Elements in Alkaline Solutions: I. Systems Pu(IV)-Fe(III) and Pu(IV)-Ni(II)." *Radiochemistry* 42(5):405–412.

– Yusov AB, NA Budantseva, AV Anan'ev, and AM Fedoseev. 2000. "Coprecipitation of Aluminum with Hydroxides of Tetra-, Penta-, and Hexavalent Actinides." *Radiochemistry* 42(5):413–416.

Guillaumont R, T Fanghänel, J Fuger, I Grenthe, V Neck, DA Palmer, and MH Rand. 2003. Page 318 of *Update on the Chemical Thermodynamics of Uranium, Neptunium, Plutonium, Americium and Technetium*. Elsevier, Amsterdam, The Netherlands.

Haire RG, MH Lloyd, ML Beasley, and WO Mulligan. 1971. "Aging of Hydrous Plutonium Oxide." *Journal of Electron Microscopy* 20(1):8–16.

Kupfer MJ, AL Boldt, KN Hodgson, LW Shelton, BC Simpson, RA Watrous, MD LeClair, GL Borsheim, RT Winward, BA Higley, RM Orme, NG Colton, SL Lambert, DE Place, and WW Schulz. 1999. *Standard Inventories of Chemicals and Radionuclides in Hanford Site Tank Wastes*. HNF-SD-WM-TI-740, Rev. 0C, Lockheed Martin Hanford Company, Richland, Washington.

Lee E, C Ribeiro, E Longo, and E Leite. 2005. "Oriented Attachment: An Effective Mechanism in the Formation of Anisotropic Nanocrystals." *Journal of Physical Chemistry B* 109:20842–20846.

Liu Y, K Kathan, W Saad, and R Prud'homme. 2007. "Ostwald Ripening of β-Carotene Nanoparticles." *Physical Review Letters* 98(3):036102-1– 036102-4.

Roetman VE, SP Roblyer, and H Toffer. 1994. *Estimation of Plutonium in Hanford Site Tanks Based on Historical Records*. WHC-EP-0793, Westinghouse Hanford Company, Richland, Washington. Available at: http://www.osti.gov/bridge/servlets/purl/10186404-mmajWH/webviewable/10186404.pdf.

Schindler PW. 1967. "Heterogeneous Equilibria Involving Oxides, Hydroxides, Carbonates, and Hydroxide Carbonates." Pages 196 to 221 of *Equilibrium Concepts in Natural Water Systems*, Advances in Chemistry Series 67, W Stumm, Symposium Chairman, American Chemical Society, Washington, D.C. (See also W Stumm and JJ Morgan. 1996. *Aquatic Chemistry – Chemical Equilibria and Rates in Natural Waters*, 3rd edition, pp. 413-414 and 806-809, John Wiley and Sons, New York.)

Shannon D. 1976. "Revised Effective Ionic Radii and Systematic Studies of Interatomic Distances in Halides and Chalcogenides." *Acta Crystallographica Section A* A32:751–767.

Shaw DJ. 1980. *Colloid and Surface Chemistry*. 3rd edition, Butterworth & Co. Ltd., New York.

Yusov AB, AYu Garnov, VP Shilov, IG Tananaev, MS Grigor'ev, and NN Krot. 2000. "Plutonium(IV) Precipitation from Alkaline Solutions. I: Effect of Precipitation and Coagulation Conditions on Properties of Hydrated Plutonium Dioxide $PuO_2 \cdot xH_2O$." *Radiochemistry* 42(2):151–156. (See also *Plutonium(IV) Precipitates Formed in Alkaline Media in the Presence of Various Anions*, NN Krot, VP Shilov, AB Yusov, IG Tananaev, MS Grigoriev, AYu Garnov, VP Perminov, and LN Astafurova. 1998. PNNL-11901, Pacific Northwest National Laboratory, Richland, Washington. Available at: http://www.osti.gov/bridge/purl.cover.jsp?purl=/665911-NwS0BW/webviewable/.)

Westrum EF, Jr. 1949. "The Preparation and Properties of Plutonium Oxides." Paper 6.57, pp. 936–944 of *The Transuranium Elements – Research Papers*, GT Seaborg, JJ Katz, and WM Manning (eds.), National Nuclear Energy Series IV-14B, McGraw-Hill Book Company, Inc., New York.

Appendix A

Derivation of Equations for the Effect of PuO_2 Particle Size on PuO_2 Solubility Product and Solubility

Appendix A

Derivation of Equations for the Effect of PuO_2 Particle Size on PuO_2 Solubility Product and Solubility

A.1 Derivation of Equation 1 and the Value of x in Equation 1

According to the derivation given by Schindler (1967), the Gibbs free energy change, ΔG, observed for the equilibrium between a massive solid, AB (S→0), with molar surface area, S, tending to zero and particle size, d, tending to infinity and a finely divided solid AB (S), of the same composition:

$$AB\ (S\rightarrow 0) \rightleftharpoons AB\ (S) \qquad \text{Reaction (1A)}$$

is related to the solubility products of the two respective AB phases by $\bar{\gamma}$, the average Gibbs free energy of the solid-liquid interface, and the molar surface area:

$$\Delta G = RT\ \ln\frac{K_{sp}^{0}(S)}{K_{sp}^{0}(S\rightarrow 0)} = \frac{2}{3}\bar{\gamma}S \qquad (1A)$$

where R is the gas constant and T is absolute temperature.

The molar surface area for particles of size d is calculated as shown in Equation (2A):

$$S = \frac{M\alpha}{\rho d} = \frac{M\times 6}{\rho d} \qquad (2A)$$

where M = formula weight of the solid
α/d = 6/d = surface area-to-volume ratio of a sphere or cube of diameter or edge length d
ρ = solid density.

Schindler (1967) derived Equation (3A) to estimate the average Gibbs free energy of the solid-liquid interface:

$$\bar{\gamma} = -\frac{3RT\ \ln K_{sp}^{0}(S\rightarrow 0)}{2N_A \sum 4\pi r_i^2} \qquad (3A)$$

where N_A is Avogadro's number and r_i are the ionic radii of the constituent ions.

Values pertinent to PuO_2 can be entered into Equations (2A) and (3A) as shown in Equations (4A) and (5A), respectively, to determine S and $\bar{\gamma}$. The PuO_2 data and other numerical values are as follows:

M = 271 g/mole PuO_2
ρ = 11.46 g/cm^3 (Clark et al. 2006)

$R = 8.314$ J/mole·degree

$T = 298$

$\log K_{sp}^{0} = -64.04$ (Guillaumont 2003)

$N_A = 6.023\times10^{23}$/mole

$r_{Pu^{4+}} = 0.096$ nm, 8-coordinate (Shannon 1976)

$r_{O^{2-}} = 0.138$ nm, 4-coordinate (Shannon 1976).

$$S = \frac{M\alpha}{\rho d} = \frac{\dfrac{271\ \text{g}}{\text{mole PuO}_2}\times 6}{\dfrac{11.46\ \text{g}}{\text{cm}^3}\times \text{d}} = \frac{141.9\ \text{cm}^3}{\text{mole PuO}_2\times \text{d}} = \frac{1.419\times10^{-4}\ \text{m}^3}{\text{mole PuO}_2\times \text{d}} \tag{4A}$$

$$\begin{aligned}\bar{\gamma} &= -\frac{3RT\ln K_{sp}^{0}(S\to 0)}{2N_A\sum 4\pi r_i^2} = \frac{3RT\ln K_{sp}^{0}(S\to 0)}{2N_A\times 4\pi\times(r_{Pu^{4+}}^2 + r_{O^{2-}}^2)}\\ &= -\frac{3\times\dfrac{8.314\ \text{J}}{\text{mol}\cdot\text{deg}}\times 298\times(-64.04)}{2\times6.023\times10^{23}\times4\pi[(0.96\times10^{-10}\ \text{m})^2 + (1.38\times10^{-10}\ \text{m})^2]}\\ &= \frac{1.113\ \text{J}}{\text{m}^2}\end{aligned} \tag{5A}$$

The values for S and $\bar{\gamma}$ from Equations (4A) and (5A) then may be entered into Equation (1A) to obtain, with algebraic rearrangement, Equation (6A):

$$\begin{aligned}\log K_{sp}^{t}(S) - \log K_{sp}^{0}(S\to 0) &= \frac{\frac{2}{3}\bar{\gamma}\,S}{2.303\,RT}\\ &= \frac{\frac{2}{3}\times\dfrac{1.113\ \text{J}}{\text{m}^2}\times\dfrac{1.419\times10^{-4}\ \text{m}^3}{\text{mole PuO}_2\ \text{d}_t}}{2.303\times\dfrac{8.314\ \text{J}}{\text{mole}\cdot\text{deg}}\times 298}\times\frac{10^9\ \text{nm}}{\text{m}}\\ &= \frac{18.46}{\text{d}_t\ (\text{nm})}\end{aligned} \tag{6A}$$

The result of Equation (6A) shows that the value of y used in Equation (1) is 18.46. Equation (6A) is used to determine the effect of particle size, d_t, on the solubility product observed for the finely divided $PuO_2{\cdot}xH_2O$ particles or, conversely, the influence of the observed solubility product on the particle size.

A.2 Derivation of Equation 4

The solubility product for PuO_2 expresses the equilibrium Reaction (2A):

$$PuO_{2\,(am,\,hydr.\,or\,cr.)} + 2\,H_2O_{\,(l)} \rightleftharpoons Pu^{4+}{}_{(aq)} + 4\,OH^-{}_{(aq)}. \qquad \text{Reaction (2A)}$$

The solubility equilibrium of the charge-neutral plutonium hydroxide dissolved species $Pu(OH)_{4\,(aq)}$ from the solid phase $PuO_{2\,(am,\ hydr.\ or\ cr.)}$ is shown in Reaction (3A):

$$PuO_{2\,(am,\ hydr.\ or\ cr.)} + 2\ H_2O_{\,(l)} \rightleftharpoons Pu(OH)_{4\,(aq)}. \qquad \text{Reaction (3A)}$$

The solubility of the $Pu(OH)_{4\,(aq)}$ solution species, $K^0_{s,4}$, is related to the $PuO_{2\,(am,\ hydr.)}$ solubility product and the cumulative formation constant of the $Pu(OH)_{4\,(aq)}$ solution species, $\beta^0_{4,1}$, by Equation (7A), which can be rearranged to Equation (8A). The analogous Equation (9A) can be written for "large crystal" $PuO_{2\,(cr)}$.

$$\log K^0_{s,4}(\text{colloid}) = \log [Pu(OH)_{4\,(aq)}] = \log (K^0_{sp}\ \text{colloid}) + \log \beta^0_{4,1} \qquad (7A)$$

$$\log (K^0_{sp}\ \text{colloid}) = \log K^0_{s,4}(\text{colloid}) - \log \beta^0_{4,1} \qquad (8A)$$

$$\log (K^0_{sp}\ \text{large crystal}) = \log K^0_{s,4}(\text{large crystal}) - \log \beta^0_{4,1} \qquad (9A)$$

Substitution of $\log (K^0_{sp}\ \text{colloid})$ and $\log (K^0_{sp}\ \text{large crystal})$ from Equations (8A) and (9A) into Equation (2) yields Equation (10A) in which the $\log \beta^0_{4,1}$ values in Equations (8A) and (9A) are identical and whose difference is zero:

$$\log K^0_{s,4}(\text{colloid}) - \log K^0_{s,4}(\text{large crystal}) = 5.71 = \frac{18.46}{d_0\ (\text{nm})} \qquad (10A)$$

The decrease in solubility of the plutonium solid (i.e., plutonium solution concentration) at any time after the highest solubility established by the ~3.2-nm size birth particle thus is reflected in the increase in size of the particle, d_t, at that later time, t. This is seen in Equation (11A), which is a recasting of Equation (10A) to include the influence of the solubility change, log Δ(solubility), for the growing colloid:

$$\log K^t_{s,4}(\text{colloid}) - \log K^0_{s,4}(\text{large crystal}) = 5.71 + \log \Delta(\text{solubility}) = \frac{18.46}{d_t\ (\text{nm})} \qquad (11A)$$

It is noted that the formation of the neutral complex $Pu(OH)_{4\,(aq)}$ becomes the first step in the subsequent dissolution equilibria needed to form the anionic hydroxide-complexed Pu(IV) and Pu(V) species postulated to form in strongly alkaline solution (e.g., $Pu(OH)_5^-$ or $PuO_2(OH)_4^{3}$, respectively; Clark and Delegard 2002). The influences of the subsequent hydroxide complexation and oxidation steps in the plutonium solute species equilibria are fixed for a given hydroxide chemical activity (NaOH concentration) and redox potential (established in Hanford tank waste by influences such as nitrate and nitrite concentration and radiolysis). Therefore, the change in the solubility equilibria established for $Pu(OH)_{4\,(aq)}$ and any subsequent dissolved species over an aging/ripening $PuO_{2\,(am,\ hydr.)}$ solid phase is reflected only in the change in the solid phase's solubility due to aging.

Appendix B

XRD Patterns of $PuO_2 \cdot xH_2O$ Precipitated from Pu(IV) and Pu(VI) Nitrate Solution in NaOH Solution

Appendix B

XRD Patterns of $PuO_2 \cdot xH_2O$ Precipitated from Pu(IV) and Pu(VI) Nitrate Solution in NaOH Solution

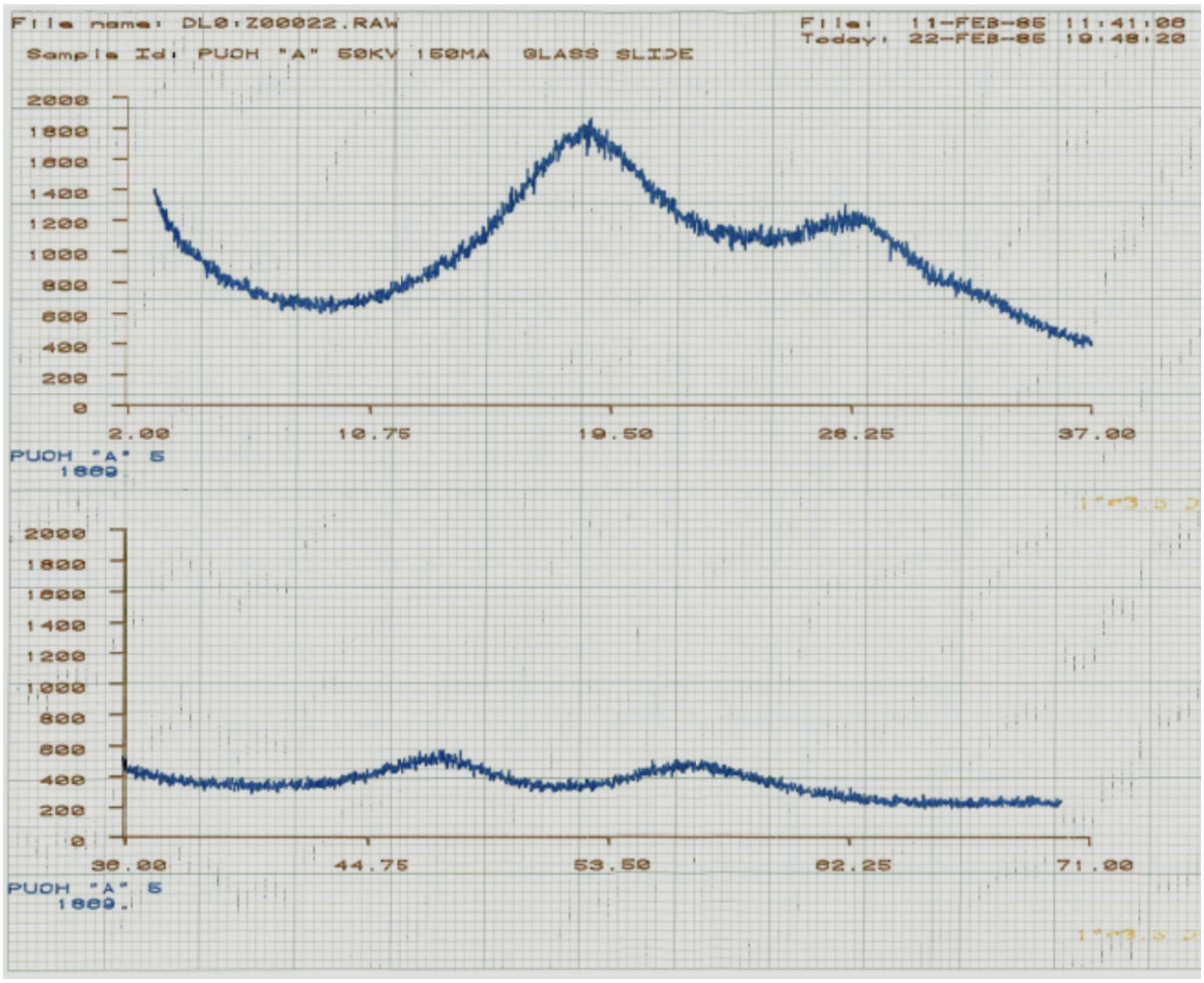

Figure B.1. XRD Pattern for $PuO_2 \cdot xH_2O$ Precipitated from Pu(IV) Nitrate in 5 M NaOH After 4 Days of Aging (full width at the half maximum of the peak at 28.55° 2-θ is 0.069 radians)

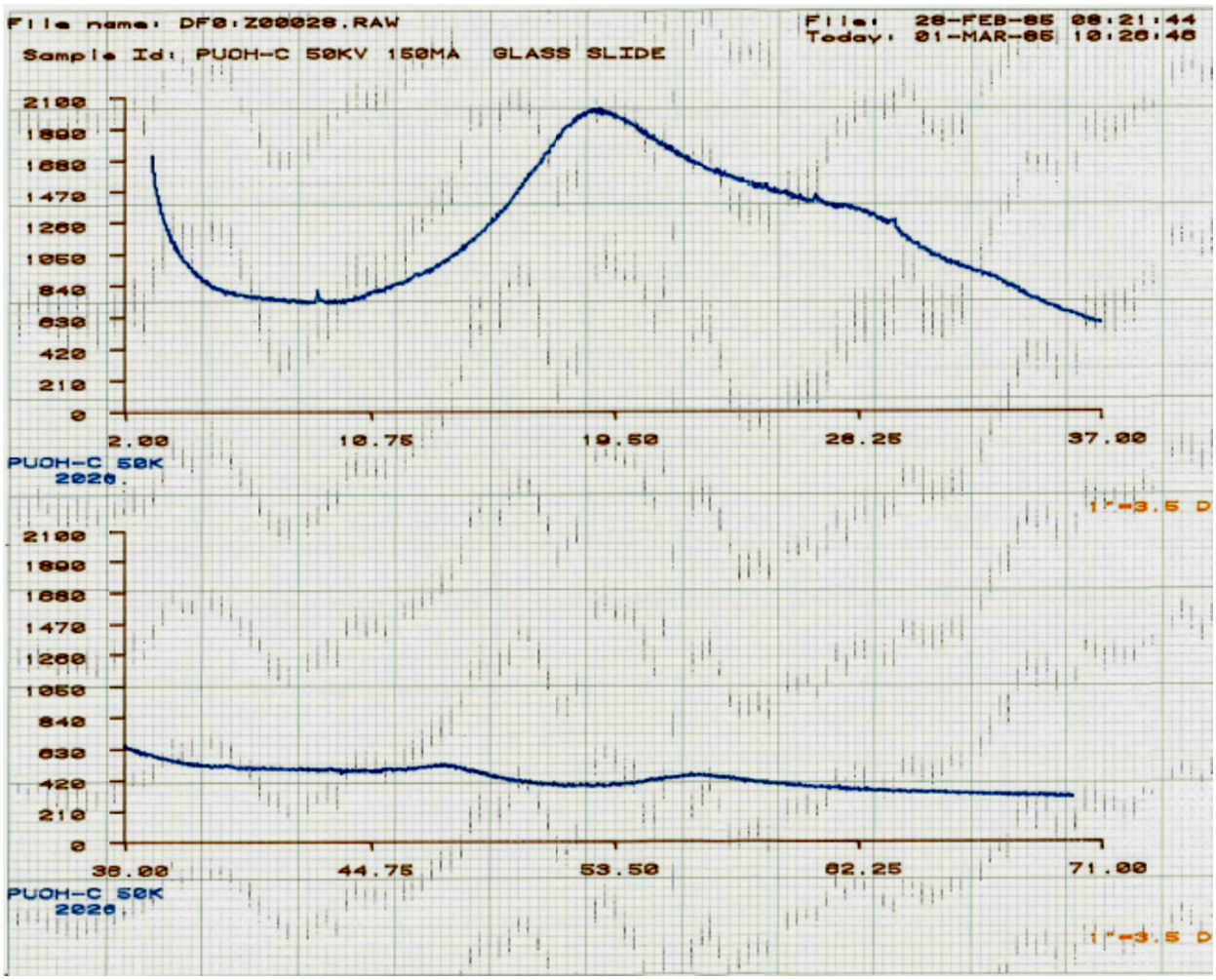

Figure B.2. XRD Pattern for $PuO_2 \cdot xH_2O$ Precipitated from Pu(IV) Nitrate in 5 M NaOH After 14 Months of Aging (full width at the half maximum of the peak at 28.55° 2-θ is 0.055 radians)

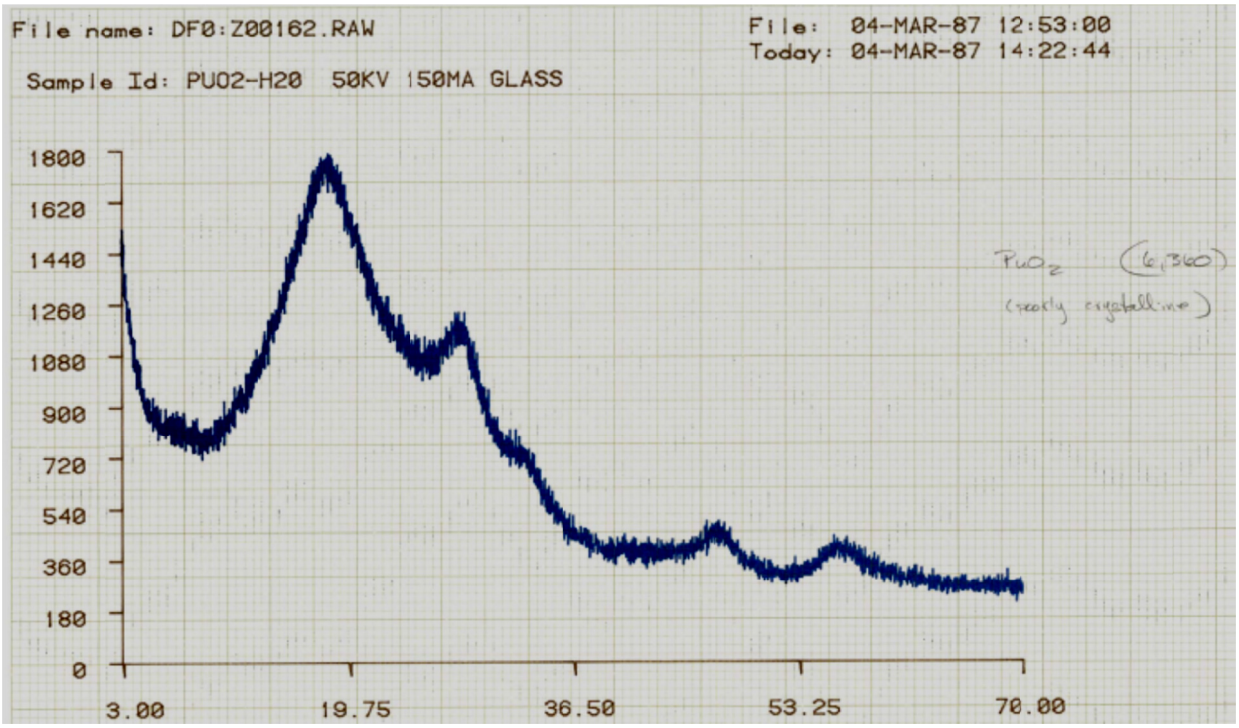

Figure B.3. XRD Pattern for $PuO_2 \cdot xH_2O$ Precipitated from Pu(IV) Nitrate in NaOH Solution After 38 Months of Aging (full width at the half maximum of the peak at 28.55° 2-θ is 0.047 radians)

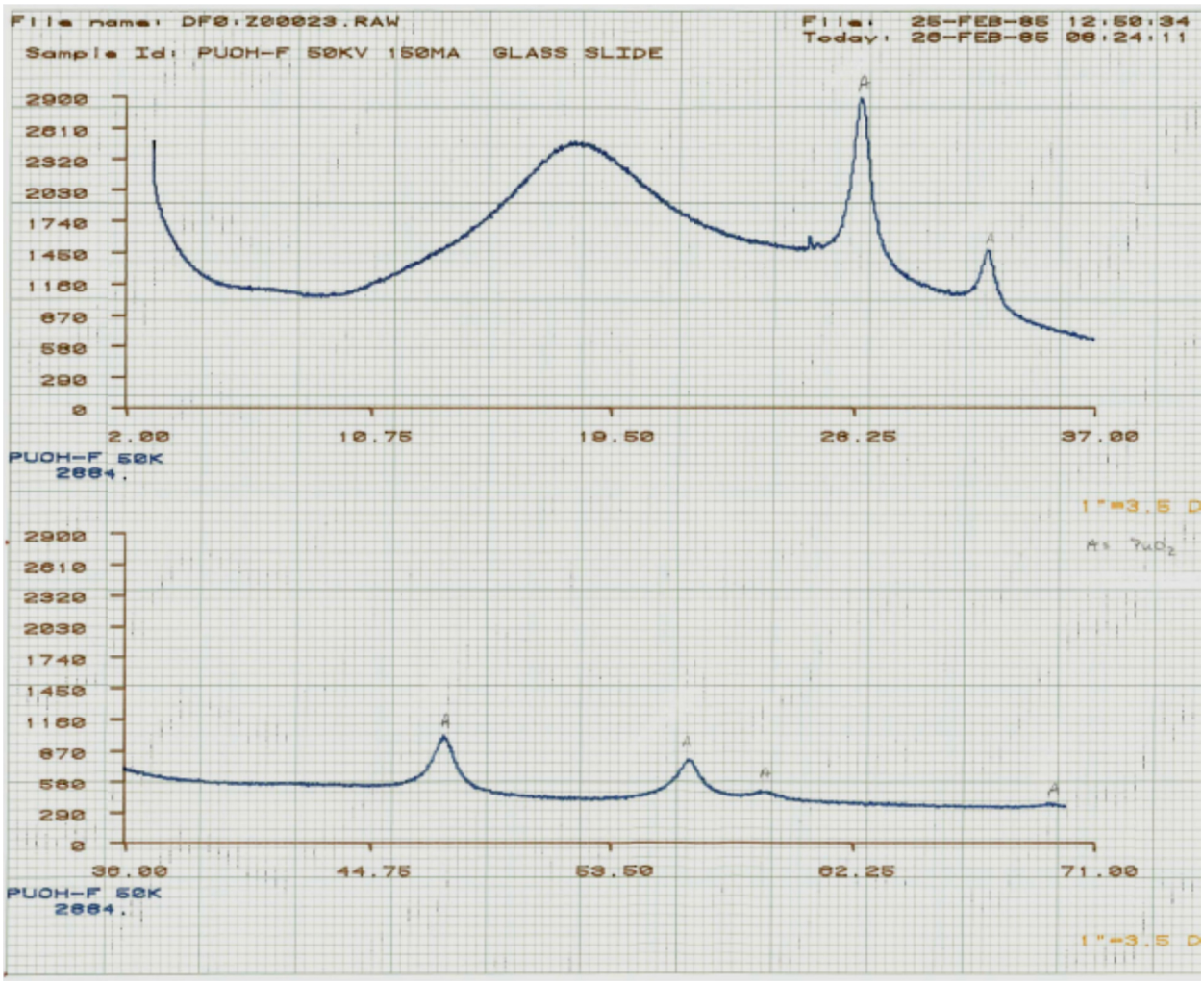

Figure B.4. XRD Pattern for $PuO_2 \cdot xH_2O$ Precipitated from Pu(VI) Nitrate in 1 M NaOH After 9½ Months of Aging (full width at the half maximum of the peak at 28.55° 2-θ is 0.0132 radians)

Appendix C

Sodium Hydroxide Solution Viscosities and Fluidities as Functions of Concentrations and Temperature

Appendix C

Sodium Hydroxide Solution Viscosities and Fluidities as Functions of Concentrations and Temperature

The dependencies of sodium hydroxide (NaOH) solution viscosities on temperature and concentration were derived from data plots compiled and published by Dow Chemical Company (Dow 2011). Values from the Dow plots were cross-checked and found to be consistent with values from other published sources. The solution fluidity, which is the inverse of the solution viscosity, is known to follow an Arrhenius dependence on temperature in which the natural logarithm of the fluidity is linearly dependent on the inverse absolute temperature with a slope of $-E_a/R$ where E_a is the activation energy of the fluidity and R is the gas constant, 8.3145 J/mole·K (Adamson 1979).

The plots of the temperature dependencies of water and NaOH solution fluidities given in Figure C.1 follow the Arrhenius equation with high fidelity over NaOH concentrations up to 40 wt% (~14.3 M) and 10 to 90°C. The E_a values for solution fluidity, taken from the slopes given in Figure C.1, are seen to increase with NaOH concentration (Figure C.2), almost doubling between pure water and 40 wt% NaOH. This means that the fluidities of the NaOH-rich Hanford tank waste solutions become increasingly temperature-dependent as the NaOH concentration increases.

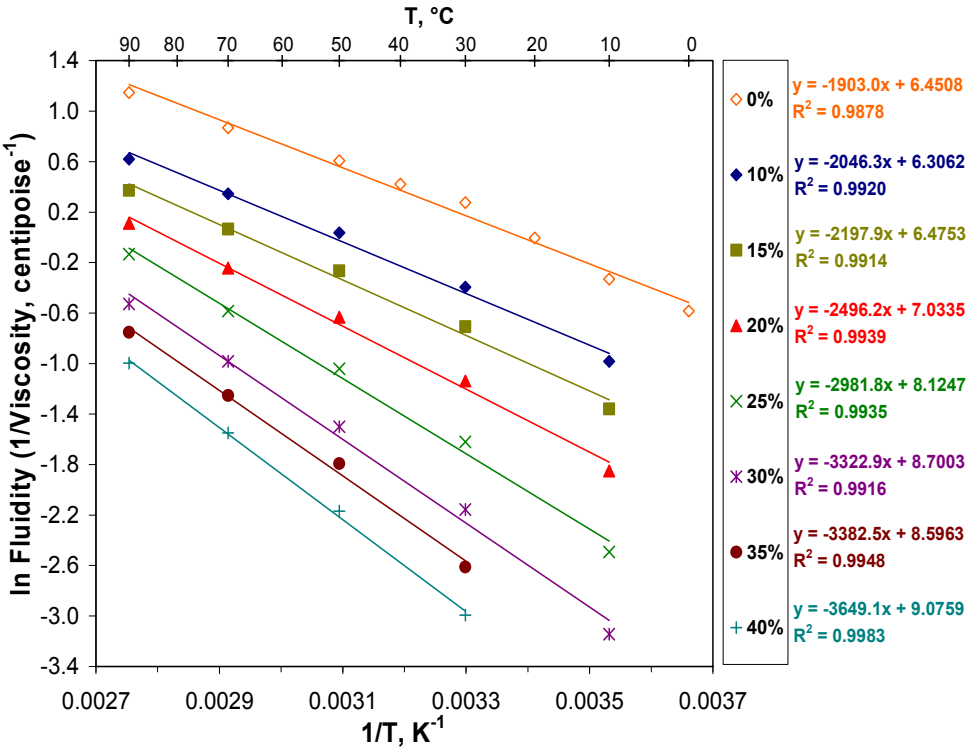

Figure C.1. Arrhenius Plot of Water and NaOH Solution Fluidities (NaOH concentrations in weight%; equations for the straight-line fits of the data are shown to the right)

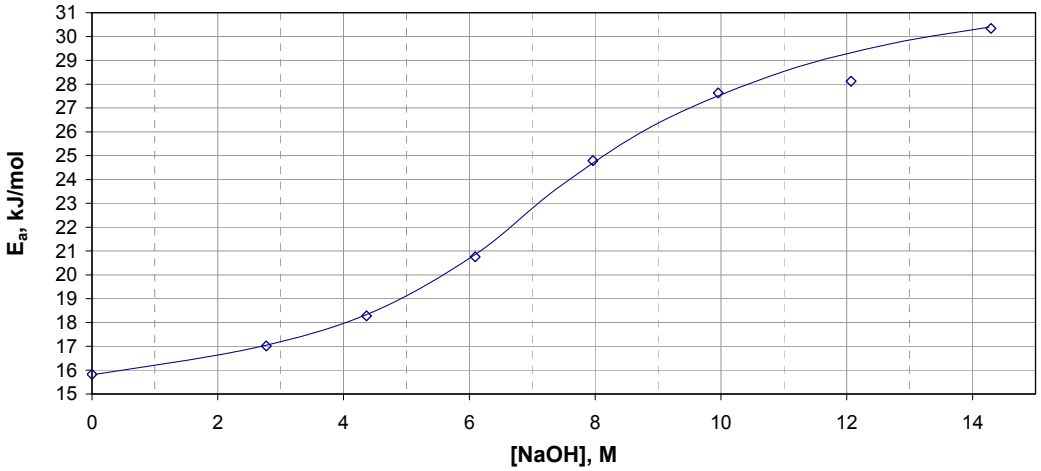

Figure C.2. Activation Energy, E_a, for Fluidity as a Function of NaOH Concentration

The multiplicative factor fluidity increases as functions of NaOH concentration and temperature shown in Figure C.3 were derived from the fluidity data to determine how much the $PuO_2 \cdot xH_2O$ crystallization rate in a given NaOH solution would increase with increasing aging temperature. For example, it is seen that the fluidity of 6 M NaOH increases by about a factor of 5 when the temperature increases from 22°C to 90°C. Therefore, the time observed for $PuO_2 \cdot xH_2O$ to grow to a given size in the room-temperature (22°C) aging tests described in Figure 2 and the related text would decrease by a factor of 5 if aging in 6 M NaOH had occurred at 90°C instead of room temperature.

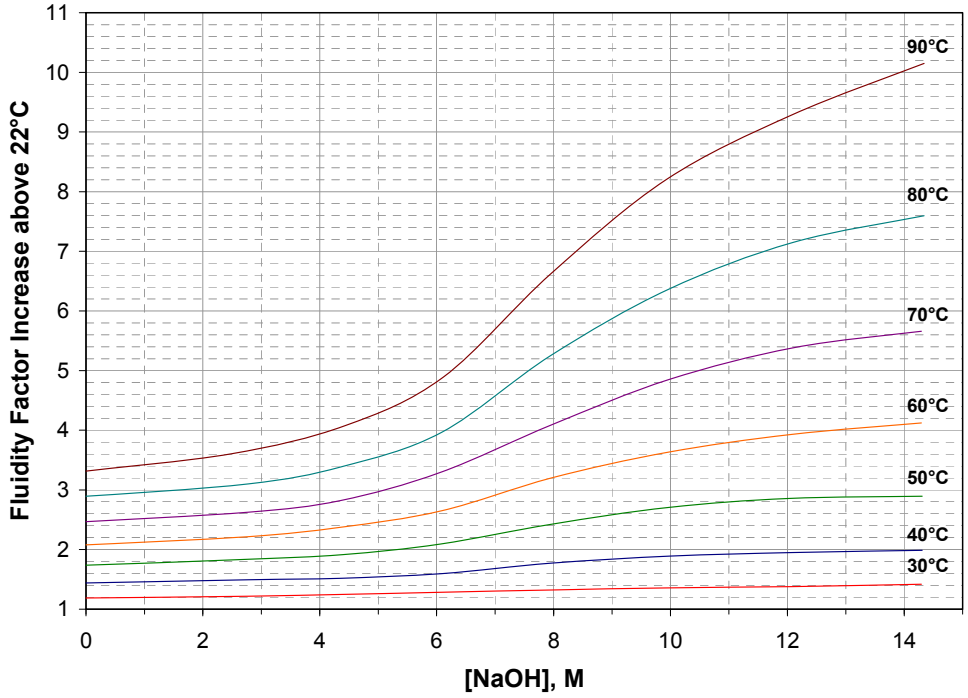

Figure C.3. Factor Increase in Fluidity Above Room Temperature (22°C) for NaOH Solution

Pacific Northwest
NATIONAL LABORATORY

Proudly Operated by Battelle *Since 1965*

U.S. DEPARTMENT OF
ENERGY

902 Battelle Boulevard
P.O. Box 999
Richland, WA 99352
1-888-375-PNNL (7665)
www.pnnl.gov